THE UNIVERSITY of EDINBURGH

Edinburgh Research Explorer

Visualization of Src activity at different compartments of the plasma membrane by FRET imaging

Citation for published version:
Seong, J, Lu, S, Ouyang, M, Huang, H, Zhang, J, Frame, MC & Wang, Y 2009, 'Visualization of Src activity at different compartments of the plasma membrane by FRET imaging' Chemistry and Biology, vol. 16, no. 1, pp. 48-57. DOI: 10.1016/j.chembiol.2008.11.007

Digital Object Identifier (DOI):
10.1016/j.chembiol.2008.11.007

Link:
Link to publication record in Edinburgh Research Explorer

Document Version:
Peer reviewed version

Published In:
Chemistry and Biology

Publisher Rights Statement:
NIH Public Access Author Manuscript

General rights
Copyright for the publications made accessible via the Edinburgh Research Explorer is retained by the author(s) and / or other copyright owners and it is a condition of accessing these publications that users recognise and abide by the legal requirements associated with these rights.

Take down policy
The University of Edinburgh has made every reasonable effort to ensure that Edinburgh Research Explorer content complies with UK legislation. If you believe that the public display of this file breaches copyright please contact openaccess@ed.ac.uk providing details, and we will remove access to the work immediately and investigate your claim.

OPEN ACCESS

Download date: 05. Apr. 2019

NIH Public Access
Author Manuscript
Chem Biol. Author manuscript; available in PMC 2010 January 30.

Published in final edited form as:
Chem Biol. 2009 January 30; 16(1): 48–57. doi:10.1016/j.chembiol.2008.11.007.

Visualization of Src activity at different compartments of the plasma membrane by FRET imaging

Jihye Seong[1], **Shaoying Lu**[2], **Mingxing Ouyang**[2], **He Huang**[2], **Jin Zhang**[4], **Margaret C. Frame**[5], and **Yingxiao Wang**[1,2,3,*]

1 *Neuroscience Program, University of Illinois, Urbana, IL 61801*

2 *Department of Bioengineering & Beckman Institute for Advanced Science and Technology, University of Illinois, Urbana, IL 61801*

3 *Department of Integrative and Molecular Physiology, Center for Biophysics and Computational Biology, University of Illinois, Urbana, IL 61801*

4 *Departments of Pharmacology and Molecular Sciences, Neuroscience, and Oncology, Johns Hopkins School of Medicine, Baltimore, MD 21205 USA*

5 *The Beatson Institute for Cancer Research, Cancer Research UK Beatson Laboratories, Garscube Estate, Switchback Road, Bearsden, Glasgow, G61 1BD, UK*

Summary

Membrane compartments function as segregated signaling platforms for different cellular functions. It is not clear how Src is regulated at different membrane compartments. To visualize local Src activity in live cells, a FRET-based Src biosensor was targeted in or outside of lipid rafts at the plasma membrane, via acylation or prenylation modifications on targeting tags either directly fused to the biosensor or coupled to the biosensor through an inducible heterodimerization system. In response to growth factors and pervanadate, the induction of Src activity in rafts was slower and weaker, dependent on actin and possibly its mediated transportation of Src from perinuclear regions to the plasma membrane. In contrast, the induction of Src activity in non-rafts was faster and stronger, dependent on microtubules. Hence, the Src activity is differentially regulated via cytoskeleton at different membrane compartments.

Keywords

FRET; Cytoskeleton; Lipid rafts; Src kinase; Imaging

Introduction

The non-receptor tyrosine kinase Src plays critical roles in numerous cellular processes (Martin, 2001). For example, Src kinase regulates cell migration by the phosphorylation of the adapter protein p130CAS to recruit Crk and DOCK180/ELMO, which can activate Rac1 to induce the formation of lamellipodia at the leading edge of migrating cells (Cote and Vuori,

*To whom correspondence should be addressed. E-mail: yingxiao@uiuc.edu Tel: 1-217-333-6727, Fax: 1-217-265-0246.

Publisher's Disclaimer: This is a PDF file of an unedited manuscript that has been accepted for publication. As a service to our customers we are providing this early version of the manuscript. The manuscript will undergo copyediting, typesetting, and review of the resulting proof before it is published in its final citable form. Please note that during the production process errors may be discovered which could affect the content, and all legal disclaimers that apply to the journal pertain.

NIH-PA Author Manuscript
NIH-PA Author Manuscript
NIH-PA Author Manuscript

NIH-PA Author Manuscript

NIH-PA Author Manuscript

NIH-PA Author Manuscript

2007; Hall, 2005; Rodriguez et al., 2003). In addition, Src binds to the autophosphorylated tyrosine 397 of focal adhesion kinase (FAK) via its SH2 domain and phosphorylates tyrosine 925 of FAK. Grb2 can then bind to this site and displaces FAK from paxillin, causing focal adhesion turnover in the trailing edge of the cell (Mitra et al., 2005). Src is also involved in the proliferation through the Ras-MAPK pathway and in cell survival through the PI3K-Akt signaling (Thomas and Brugge, 1997). To mediate such a variety of cellular signaling transduction, the activation and function of Src kinase require a highly coordinated regulation in space and time. Indeed, Src at resting state was shown to localize mainly in the endosomes near perinuclear region and microtubule organizing center (MOTC) (Kaplan et al., 1992). Upon stimulation, active Src can be translocated to the plasma membrane via the actin cytoskeleton (Sandilands et al., 2004). There is also evidence that Src regulates down-stream signals differently depending on its subcellular localization. For example, Src induces the p190RhoGAP activation and subsequently inhibits RhoA at the focal adhesion sites (Thomas and Brugge, 1997), but activates RhoA at podosomes (Berdeaux et al., 2004). Therefore, the visualization of the dynamic activation pattern of Src at subcellular environments will provide critical insights on our understanding of the molecular mechanism regulating cellular functions.

The plasma membrane is not uniform in structure (Simons and Toomre, 2000) and has different nano-size compartments, e.g. lipid rafts, which are rich in cholesterol, sphingomyelin, and saturated fatty acids (Brown and Rose, 1992). These compartmental structures are involved in the localization and regulation of intracellular signaling molecules (Jacobson et al., 2007; Lasserre et al., 2008). For example, Src family kinases (SFKs) have been shown to be transported to distinct compartments of plasma membrane through different types of endosomes (Sandilands et al., 2007). SFK members such as Lyn and Fyn can reside in lipid rafts of the plasma membrane (Simons and Toomre, 2000), via their N-terminal sequences after myristoylation and palmitoylation (Zacharias et al., 2002). However, Src kinase has only myristoylation motif and it remains controversial whether Src kinase localizes within lipid rafts at the plasma membrane (Arcaro et al., 2007; Hitosugi et al., 2007; Hur et al., 2004; Kasai et al., 2005; Mukherjee et al., 2003; Shima et al., 2003). The detergent extraction method has been widely used to study the lipid rafts based on its detergent-resistant property. In mouse fibroblasts, Src was shown to be excluded from the detergent-resistant membrane (DRM) fractions in one study while another publication suggested that Src resides in DRM fraction (Mukherjee et al., 2003; Shima et al., 2003). Different groups also reported different Src localizations in PC12 cells (Hur et al., 2004; Kasai et al., 2005). This inconsistency is likely attributed to the controversial effects of non-ionic detergents used in these reports for isolating DRMs, which, however, may not exactly correspond to lipid rafts in living cells and may include membranes that do not contain rafts before detergent extraction (Lichtenberg et al., 2005; Shaw, 2006). Thus, the development of advanced methods is required to study the lipid rafts in live cells.

Previous studies have shown that genetically-encoded biosensors, based on fluorescence resonance energy transfer (FRET), are capable of monitoring various cellular events in live cells with high spatial and temporal resolution (Zhang et al., 2002). We have previously developed a Src FRET biosensor which can detect Src activity in the cytoplasm (Wang et al., 2005). In this study, this Src FRET biosensor was further coupled to membrane-targeting motifs, either by direct fusion or by an inducible heterodimerization system. As such, the biosensor can be directed to tether at different compartments of plasma membrane, where the local Src activity in live cells can be monitored and quantified in real time. Our results revealed that the Src activity is differentially regulated at different compartments of the plasma membrane, mediated by different sets of cytoskeletal components.

NIH-PA Author Manuscript

NIH-PA Author Manuscript

NIH-PA Author Manuscript

Results

A faster and stronger induction of Src activity at non-raft membrane compartments

We have previously developed a FRET biosensor capable of visualizing the spatiotemporal Src activity in live cells (Wang et al., 2005). To monitor the local Src activity in different compartments at the plasma membrane, this Src FRET biosensor was genetically modified to be tethered in or outside of lipid rafts (Supplementary Fig. 1). It has been shown that lipid modification, e.g. acylation and prenylation, is sufficient to target the proteins into the different microdomains of plasma membrane (Zacharias et al., 2002). The lipid raft-targeting biosensor (Lyn-Src biosensor) was hence constructed by genetically fusing acylation substrate sequences derived from Lyn kinase to the N-terminus of the cytosolic Src biosensor (Wang et al., 2005). N-terminal glycine and cysteine in the acylation sequences can undergo myristoylation and palmitoylation (Resh, 1994), which partition the biosensor into lipid rafts (Simons and Toomre, 2000). The non-raft biosensor (KRas-Src biosensor) was developed by introducing prenylation sequences (KKKKKKSKTK**C**VIM) from KRas to the C-terminus of the cytosolic Src biosensor. Prenylation on the C-terminal cysteine residue and the neighboring polybasic amino acids can target the biosensor to the non-raft regions (Zacharias et al., 2002). In fact, different mobilization properties of Src biosensors in the microdomains of the plasma membrane have been revealed in our recent publication using fluorescence recovery after photobleaching (FRAP) analysis (Lu et al., 2008). We have further conducted the *in vitro* kinase assay to examine the cytosolic, Lyn- and Kras-tagged biosensors. The results revealed that the responses of these three biosensors are very similar in kinetics and magnitude upon Src phosphorylation (Data not shown), suggesting that these modifications of Src biosensor by fusing peptides at N/C terminus do not affect its function in reporting Src activity. Therefore, FRET changes of the Lyn- and Kras-Src biosensors can be used to monitor the Src activity at different compartments of the plasma membrane.

To investigate the spatiotemporal induction of Src activity, we first examined the FRET response of different Src biosensors in response to growth factor stimulations (Fig. 1). The results revealed that both epidermal growth factor (EGF, 50 ng/ml) in HeLa cells and platelet-derived growth factor (PDGF, 50 ng/ml) in mouse embryonic fibroblasts (MEFs) induced significant FRET changes of the Src biosensors, with a faster and stronger response from the non-raft KRas-Src biosensor when compared to that of the Lyn-Src biosensor at rafts (Fig. 1, Movies S1 and 2). In fact, the non-raft KRas-Src biosensor responded promptly to reach the peak (50–60% change) within 3–5 min, whereas the response of raft Lyn-Src biosensor was much slower and weaker (10–20% change). These results suggest a faster and stronger induction of Src activity in non-raft regions at the plasma membrane upon growth factor stimulations.

Recent evidence suggests that growth factors may regulate signaling transduction via the activation of receptors as well as the generation of reactive oxygen species (ROS) such as H_2O_2, which oxidize cysteine residues and subsequently inhibit protein tyrosine phosphatases (PTPs) (Rhee, 2006). The reactive oxygen species have also been shown to enhance the Src activity (Boulven et al., 2002; Huyer et al., 1997; Takahashi et al., 2004). This combined effect of phosphatase inhibition and Src kinase activation by ROS can highlight Src phosphorylation efficiency on the biosensors to cause their FRET change. Hence, the differential induction of Src activity at different compartments of the plasma membrane was then examined using a ROS generator pervanadate (PVD, 20 μM), which inhibits tyrosine phosphatases and activates Src kinase (Boulven et al., 2002). Again, the KRas-Src biosensor in HeLa cells showed a much faster and stronger FRET change in comparison to the Lyn-Src biosensor (Fig. 2A, Movie S3). The CFP/YFP ratio of Lyn-Src biosensor starts to increase around 15 min after PVD application when that of KRas-Src biosensor had already reached its peak. These significantly distinct time courses in FRET response of the KRas- and Lyn- Src biosensors suggest that raft- and non-

NIH-PA Author Manuscript

NIH-PA Author Manuscript

NIH-PA Author Manuscript

raft-associated proteins are possibly separated or exchangeable but stay at the different microdomains with different resident time (Malinska et al., 2003; Zacharias et al., 2002). Similar difference in the responses of the KRas- and Lyn-Src biosensors was also observed in other cell types, including bovine aortic endothelial cell (BAEC) and mouse embryonic fibroblast (MEF) (Supplementary Fig. 2). These PVD-induced FRET changes of Src biosensors were inhibited in SYF−/− MEF cells (null in Src family kinases: Src, Yes, and Fyn) or after the pretreatment of Src inhibitor PP1 (20 μM) in HeLa cells (Supplementary Fig. 3), confirming that the PVD-induced FRET responses mainly represent the enhanced Src activities. These results suggest that a faster and stronger enhancement of Src activity occurred in non-raft regions at the plasma membrane.

Quantification of the kinetics and magnitude of the FRET responses of Src biosensors

To further study the different kinetics of the Src phosphorylation efficiency upon PVD in membrane compartments, we quantified the parameters representing the Src activation kinetics based on the velocity curves of FRET change in time. The velocity of FRET change, v_i, was calculated by taking the discrete time derivatives of the normalized CFP/YFP emission ratios. The resulting bell-shaped velocity curves were fitted by the Gaussian functions given by the equation

$$v(t)=A\cdot\frac{1}{\sqrt{2\pi}\sigma}\cdot\exp\left(-\frac{(t-\mu)^2}{2\sigma^2}\right).$$

The parameters A, σ, and μ, were estimated by parameter fitting to represent the total FRET change, reaction duration, and the time point where the reaction reaches the maximal velocity, respectively. The onset time of the reaction, T_0, was calculated based on the values of σ and μ ($T_0 = \mu - 1.64485\times\sigma$ see Supplementary materials). The mean and standard deviation of the parameters were calculated using data from multiple cells and compared between different groups.

The KRas-Src biosensor, in comparison to the Lyn-Src biosensor, showed significantly higher value in A (KRas-Src: 0.5734±0.0122; Lyn-Src: 0.3381±0.0088), representing a stronger response, and lower values in σ (KRas-Src: 2.058±0.1169; Lyn-Src: 2.441±0.1459) and T_0 (KRas-Src: 6.936±0.6320; Lyn-Src: 14.042±0.1942), indicating faster and earlier responses (Fig. 2C and Supplementary Table 1). These statistical results confirmed the FRET observations obtained from single-cell imaging. The different dynamics of compartment-targeted Src biosensors was further verified by immunoprecipitation/immunoblotting. As shown in Supplementary Fig. 4, the phosphorylation of the KRas-Src biosensor caused by the enhanced Src activity was detected earlier than that of the Lyn-Src biosensor upon PVD stimulation.

Inducible heterodimerization system

The membrane-anchoring motif for the Lyn-Src biosensor is at the N-terminus whereas it is at the C-terminus for the KRas-Src biosensor (Supplementary Fig. 1). To exclude the possibility that different responses of biosensors were caused by different tagging motifs and/or 3D orientations of the biosensors in relation to the plasma membrane, we applied an inducible heterodimerization system for the membrane localization (Inoue et al., 2005) (Fig. 3A). The cytosolic Src biosensor was fused to the FRB domain, and the Lyn- or KRas-targeting motif was fused to FKBP (FRB binding peptides) (Supplementary Fig. 1). When a heterodimerizer AP21967 (1 μM) was introduced into HeLa cells expressing FRB-Src biosensor and the Lyn- or Kras-FKBP peptide, the cytosolic FRB-Src biosensor was successfully recruited to the Lyn-

NIH-PA Author Manuscript

NIH-PA Author Manuscript

NIH-PA Author Manuscript

or KRas-FKBP peptides located at the plasma membrane (Fig. 3B and Movie S4, Data not shown). Again, the subsequent addition of PVD induced a faster and stronger FRET response of the FRB-Src biosensor dimerized with KRas-FKBP than that with Lyn-FKBP (Fig. 3C). Statistical results further revealed that the KRas-FKBP/FRB-Src biosensor has higher *A* and lower σ values, in comparison to the Lyn-FKBP/FRB-Src biosensor (Supplementary Table 1). These results verified that the different kinetics of KRas- and Lyn-Src biosensors originate from their differential compartmental localization, but not from different tagging motifs, nor 3D orientations.

Two distinct populations of Src kinases are regulated by different cytoskeletal components

The plasma membrane is directly connected with and mechanically supported by cytoskeletal structures such as polymerized actin and microtubule filaments (Etienne-Manneville, 2004; Rodriguez et al., 2003; Warner et al., 2006). The cytoskeleton has also been known to play important roles in the intracellular movement of molecules, in particular, Src translocation (Sandilands et al., 2007; Sandilands et al., 2004). Thus, we examined the role of the cytoskeletal network in regulating the localization and activation of Src kinase at different membrane compartments.

Since it has been shown that Src kinase can be transported to the plasma membrane via the actin network upon growth factor stimulation (Fincham et al., 1996), we monitored the mobilization of Src kinase (Fig. 4A, upper panels and Movie S6) and actin dynamics upon PVD application (Fig. 4A, lower panels) using EGFP-conjugated c-Src kinase (Sandilands et al., 2004) and mCherry-conjugated β-actin (Shaner et al., 2004). At the resting state, a large population of Src kinases can be clearly observed near perinuclear region within endosome-like structures as previously reported (Sandilands et al., 2004). At 10 min after PVD application, the Src concentration started to decrease in perinuclear regions, with a concomitant increase at cell periphery and plasma membrane ruffles. A co-localization of Src kinase and actin can also be observed at the cell periphery regions after PVD stimulation (Fig. 4A). These results suggest that Src kinase may be transported to plasma membrane by actin filaments upon PVD stimulation. Indeed, after the pretreatment of cytochalasin D (CytoD) for 1 hr to block actin polymerization, the redistribution of EGFP-wt Src upon PVD was not observed (Supplementary Fig. 5, left panels). The membrane-translocation of Src kinase was also blocked by co-transfection of Scar1 WA (a dominant negative mutant of Scar1), which inhibits actin nucleation (Supplementary Fig. 5, middle panels). Interestingly, the inhibition of microtubule by nocodazole (Noco) did not significantly affect the redistribution of c-Src kinase into cell peripheral regions (Supplementary Fig. 5, right panels). These results suggest that Src kinases can translocate to the plasma membrane by utilizing the actin cytoskeleton upon PVD stimulation, similar to previous observations in cells subjected to growth factor stimulation (Fincham et al., 1996).

We then investigated the relationship between different cytoskeletal networks and the responses of Src biosensors (Fig. 4B–E). The PVD-induced FRET response of the Lyn-Src biosensor was significantly inhibited by 1 hr of pretreatment with CytoD (1 μM), but not with 1 μM Noco (Fig. 4B and 4D, Supplementary Fig. 6A and Supplementary Table 1). CytoD increased the duration of the reaction (σ increased from 2.441±0.1459 to 4.474±0.4830) and decreased total FRET change (*A* decreased from 0.3381±0.0088 to 0.2049±0.0366) of the Lyn-Src biosensor, suggesting a slower and weaker response (Fig. 4B and Supplementary Table 1). These results suggest that the PVD-induced Src activation at lipid rafts is dependent on actin, likely through the Src translocation to the plasma membrane mediated by actin, but not microtubules.

In contrast to the Lyn-Src biosensor, the PVD-induced rapid response of the KRas-Src biosensor was independent of the membrane-translocation of perinuclear Src kinases. The

NIH-PA Author Manuscript

NIH-PA Author Manuscript

NIH-PA Author Manuscript

disruption of actin filaments, which blocked the membrane-translocation of Src kinase (Supplementary Fig. 5), did not show significant inhibitory effects on the response of the KRas-Src biosensor (Fig. 4C and 4E, and Supplementary Table 1). In fact, the KRas-Src biosensor started to respond at around 5 min (Fig. 2A), well before a significant translocation of Src kinases can be observed (Fig. 4A). Interestingly, the non-raft Src activity was dependent on microtubules, because the pretreatment with Noco caused a significantly delayed (T_0 increased from 6.936±0.6320 to 14.263±0.9240) and slower (σ increased from 2.058±0.1169 to 5.023 ±0.7430) response of the KRas-Src biosensor upon PVD treatment (Fig. 4C and Supplementary Table 1). Taxol, a reagent stabilizing microtubules and hence perturbing the dynamics of microtubules, showed similar effects as Noco on the non-raft KRas-Src biosensor (Data not shown). The total change of CFP/YFP ratio *A* for the KRas-Src biosensor was not significantly affected by Noco treatment (Fig. 4C and Supplementary Table 1), suggesting that microtubule may affect the onset time and speed, but not the total magnitude of the non-raft Src activation.

We have further examined the roles of microtubules and actin cytoskeleton in regulating the responses of the cytosolic Src biosensor. The results revealed that the disruption of neither actin cytoskeleton nor microtubules inhibited the FRET response of cytosolic Src biosensor upon PVD stimulation (Data not shown). These results suggest that the inhibitory effect of cytoskeletal disruption is specific for the membrane-targeted biosensors and that the phosphorylation of Src biosensor in the cytoplasm does not require an intact cytoskeleton upon PVD stimulation. Thus, the cytoskeleton may be important for the regulation of Src functions at the plasma membrane, but not necessary so for the cytosolic processes.

Discussion

Proper subcellular localization of signaling molecules and interaction with correct target molecules are important characteristics of coordinated regulation of the complex signaling network and physiological functions. For example, Src induces the p190GAP activation and inhibits Rho GTPase at the focal adhesion sites (Thomas and Brugge, 1997), whereas it activates Rho GTPase at podosomes (Berdeaux et al., 2004). Lipid rafts have been suggested to serve as the integration site for a variety of signaling pathways. The localization of small GTPase TC10 at lipid rafts is required for the insulin-induced activation and the subsequent regulation of glucose transporter (GLUT) 4 (Watson et al., 2001). Akt in or outside of lipid rafts responded differently to PDGF but not to IGF-1 (Gao and Zhang, 2008). Src kinase also appears to be recruited into lipid rafts by Cbp and inhibited by Csk (Oneyama et al., 2008). Due to the controversial effects of detergent-based extraction of rafts-associated proteins, contradictory results have been reported on the roles of rafts or membrane compartments in determining the Src functions (Arcaro et al., 2007; Hitosugi et al., 2007; Hur et al., 2004; Kasai et al., 2005; Mukherjee et al., 2003; Shima et al., 2003).

In this paper, we developed a novel non-invasive method, combining FRET biosensor and statistical analysis, to study the Src activity in live cells at different compartments of plasma membrane. Our results indicate that the Src activity at the plasma membrane outside of lipid rafts is enhanced in a faster and stronger fashion upon the application of growth factors and PVD. Together with the previous observations that, at resting state, Src kinase is concentrated at the plasma membrane outside of DRM regions (Hitosugi et al., 2007; Kasai et al., 2005; Mukherjee et al., 2003) and at cytoplasm in perinuclear endosomes (Sandilands et al., 2007; Sandilands et al., 2004), our results support the model of two distinct populations of Src (Fig. 5). One population of Src kinase exists in non-raft regions on the plasma membrane at the resting state and can be rapidly activated upon stimulation (Hitosugi et al., 2007; Kasai et al., 2005; Mukherjee et al., 2003). The other population of Src is located in perinuclear endosomes at the resting state, and can be transported to lipid rafts upon stimulation in an actin-dependent manner. These differentially regulated Src may direct different cellular functions. Indeed, v-

NIH-PA Author Manuscript

NIH-PA Author Manuscript

NIH-PA Author Manuscript

Src at different subcellular locations has been recently reported to regulate differential signaling pathways. For example, v-Src was found at both raft and non-raft regions upon thermoactivation to regulate PI3K/Akt and MAPK/ERK pathways, respectively (de Diesbach et al., 2008). Interestingly, the raft-anchored Akt biosensor has been shown recently to have a faster and stronger response upon PDGF stimulation than that in non-raft regions (Gao and Zhang, 2008). This result suggests that the raft-localization facilitates the Akt activation. Together with our observations that Src kinase functions more strongly in non-raft regions at the plasma membrane, it is clear that cells can coordinate the molecular functions and network by controlling the subcellular localization of molecules.

Our results further suggest that these distinct responses of membrane-targeted Src biosensors are mediated by different cytoskeletal networks. The disruption of microtubules had significant effects on the early non-raft Src activation without affecting the translocation and activation of Src at rafts (Fig. 4C and E, Supplementary Fig. 5), whereas the blockade of actin polymerization by CytoD significantly inhibited the membrane translocation of Src and its activity at lipid rafts (Fig. 4B and D, Supplementary Fig. 5). Our results suggest the model that Src activation at rafts may be dependent on the transportation of Src kinases from perinuclear regions to the plasma membrane by actin cytoskeleton, although there is a possibility that actin depolymerization also affects other cellular processes in regulating Src activation. This model is supported by the previous observation that Src can be transported from perinuclear endosome-like regions to cell membrane via actin cytoskeleton and becomes highly activated (Sandilands et al., 2004). In fact, there is ample evidence that lipid rafts are closely connected to actin cytoskeleton. For example, actin-binding proteins such as ezrin and filaminA can serve as bridges between actin cytoskeleton and raft-associated protein such as PAG1 and CD28 (Viola and Gupta, 2007). The raft-associated phosphoinositide lipid PI(4,5)P_2 was also shown to regulate actin dynamics by recruiting actin-regulatory molecules such as WASP and ERM (Caroni, 2001). Indeed, actin depolymerization by Latrunculin B blocks the proper localization and simulation-induced clustering of raft-anchored fluorescent probes or H-Ras molecules (Chichili and Rodgers, 2007; Murakoshi et al., 2004). The treatment of CytoD to disrupt actin filaments also prevented proper interactions between raft-associated Lyn and IgE-FcεRI (Holowka et al., 2000).

Interestingly, a negative mutant of Scar1 (WA) blocked the responses of both KRas- and Lyn-Src biosensor upon PVD (Data not shown). We reasoned that there may be a slow chronic recycling process to maintain the pre-stored Src population at the plasma membrane outside of lipid rafts (Maxfield and McGraw, 2004), which is dependent on actin-mediated membrane-transportation. The long-term (48 hr) inhibition of actin nucleation by Scar1 WA may block the membrane-transportation and prevent an accumulation of Src at the plasma membrane in and outside of lipid rafts, resulting in the inhibition of both the Lyn- and KRas-Src biosensors. It is possible that Src kinases are initially transported to lipid rafts and then translocate into non-raft regions to form the pre-stored Src population. The short-term (1 hr) treatment of CytoD may only block the acute membrane-translocation of Src toward lipid rafts, but did not affect the pre-stored Src outside of lipid rafts. Hence, CytoD significantly inhibited the response of Lyn-Src, but not that of KRas-Src biosensor (Fig. 4B–E).

Significance

In contrast to the traditional *in vitro* assays performed in test tubes and cuvettes, the integration of FRET and specific membrane-targeting biosensors allows the quantification of the parameters of enzymatic reactions such as T_0, A, and σ in compartments of plasma membrane, whose sizes are smaller than the resolution of conventional optical fluorescence microscope (e.g. the size of single lipid raft is believed to be around 50 nm) (Pralle et al., 2000). The velocity of FRET response in the membrane compartment of each individual cell fits well with the bell-

NIH-PA Author Manuscript

NIH-PA Author Manuscript

NIH-PA Author Manuscript

shaped Gaussian function. This result indicates that enzymatic reactions in these different compartments are relatively complex and different from the instant-onset enzymatic reaction described by the Michaelis–Menten model *in vitro*. These FRET analysis assays can hence advance our systematic and in-depth understanding of enzymatic reactions at subcellular compartments in live cells. The curve fitting and statistical analysis method also provides a general platform to integrate a large quantity of data from single-cell FRET images for the quantification of the molecular kinetics of different signaling cascades. In combination to this statistical analysis approach, our FRET biosensors and live-cell imaging techniques can provide a robust and non-intrusive alternative to the biochemical assays.

Experimental Procedures

Cell Culture and Reagents

HeLa, Mouse embryonic fibroblast (MEF) cells were purchased from ATCC. The *Src*/*Fyn*/*Yes* triple knockout MEF (SYF −/−) was a generous gift from Dr. Jonathan Cooper, Fred Hutchinson Cancer Research Center. Bovine aortic endothelial cells (BAECs) were isolated from bovine aorta with collagenase. Cell culture reagents were obtained from Invitrogen. Cells were maintained in Dulbecco's modified Eagle medium (DMEM) supplemented with 10% fetal bovine serum (FBS), 2 mM L-glutamine, 1 unit/ml penicillin, 100 μg/ml streptomycin, and 1 mM sodium pyruvate. Cells were cultured in a humidified 95% air, 5% CO_2 incubator at 37°C.

Actin filaments or microtubules were disrupted by incubation for 1 hr with cytochalasin D (Sigma; 1 μM) or nocodazole (Sigma; 1 μM), respectively (Wang et al., 2005). Epidermal growth factor (EGF) and platelet-derived growth factor (PDGF) were purchased from Sigma.

DNA Constructions and Plasmids

The Lyn-Src biosensor was previously developed and described (Wang et al., 2005). The KRas-Src biosensor was constructed by fusing 14 KRas-prenylation sequences (KKKKKKSKTKCVIM) to the C-termini of Src biosensor using polymerase chain reaction (PCR). For the FRB-Src biosensor, PCR was applied to create *Hind*III and *BamH*I sites flanking FRB. The PCR product was fused to the N-termini of Src biosensor in pcDNA3 (Invitrogen). Lyn-FKBP or KRas-FKBP was constructed by PCR of FKBP with Lyn-acylation sequence (Wang et al., 2005) incorporated into the sense primer or KRas-prenylation sequence into the anti-sense primer, respectively. The PCR products of Lyn- or KRas-FKBP were inserted into pcDNA3 using *EcoR*I/*Hind*III restriction enzyme sites.

mCherry-β-actin was a kind gift from Dr. Roger Y. Tsien, University of California, San Diego. The expression of mCherry-actin, Scar1WA, and EGFP-wt Src was previously described (Sandilands et al., 2004; Shaner et al., 2004).

Preparation of Pervanadate

Pervanadate solution was prepared as previously described (Huyer et al., 1997). In brief, 10 μl of 100 mM Na_3VO_4 and 50 μl of 0.3% H_2O_2 in 20 mM HEPES (pH 7.3) were mixed in 940 μl of H_2O. After 5 min, catalase (CalBiochem, 260 units/ml) was added to release excess H_2O_2, which resulted in 1 mM pervanadate.

Inducible Heterodimerization System

The ARGENT™ regulated heterodimerization kit was obtained from ARIAD Pharmaceuticals, Inc. The dimerization domain FKBP was conjugated to Lyn-acylation (Wang et al., 2005) or KRas-prenylation sequences for membrane targeting. The other dimerization domain FRB was conjugated to the cytosolic Src biosensor. The cells were co-transfected with the FRB-

NIH-PA Author Manuscript

NIH-PA Author Manuscript

NIH-PA Author Manuscript

conjugated Src biosensor and a membrane-targeted FKBP domain (either KRas-FKBP or Lyn-FKBP). Upon the addition of rapamycin analogue AP29167 (1 μM), the FRB-conjugated Src biosensor can be induced to associate with the membrane-bound FKBP and be targeted to different compartments at plasma membrane.

Image Acquisition

During imaging, the cells were cultured in cover-glass-bottom dishes and maintained in 0.5% FBS CO_2-independent medium (Gibco BRL) at 37°C. Images were collected by a Zeiss Axiovert inverted microscope and a cooled charge-coupled device (CCD) camera (Photometrics, Tucson, AZ) using MetaFluor 6.2 software (Universal Imaging) with a 420DF20 excitation filter, a 450DRLP dichroic mirror, and two emission filters controlled by a filter changer (475DF40 for CFP and 535DF25 for YFP). The mCherry-β-actin images were collected using a 560DF40 excitation filter, a 595DRLP dichroic mirror, and a 653DF95 emission filter. A neutral density filter was used to control the intensity of the excitation light. The fluorescence intensity of non-transfected cells were quantified as the background signals and subtracted from the CFP and YFP signals on transfected cells. The pixel-by-pixel ratio images of CFP/YFP were calculated based on the background-subtracted fluorescence intensity images of CFP and YFP by the MetaFluor program to allow the quantification and statistical analysis of FRET responses by Excel (Microsoft) and Matlab (The MathWorks). The emission ratio images were shown in the intensity modified display (IMD) mode (Wang et al., 2005).

Supplementary Material

Refer to Web version on PubMed Central for supplementary material.

Acknowledgements

We are very grateful to Dr. Roger Y. Tsien for mCherry cDNA. This work was supported in part by grants from Wallace H. Coulter Foundation and Beckman Laser Institute, Inc. (Y.W.), NIH grants DK073368 and CA122673, and an AHA award 0530217N (J. Z.).

References

Arcaro A, Aubert M, Espinosa del Hierro ME, Khanzada UK, Angelidou S, Tetley TD, Bittermann AG, Frame MC, Seckl MJ. Critical role for lipid raft-associated Src kinases in activation of PI3K-Akt signalling. Cell Signal 2007;19:1081–1092. [PubMed: 17275257]

Berdeaux RL, Diaz B, Kim L, Martin GS. Active Rho is localized to podosomes induced by oncogenic Src and is required for their assembly and function. J Cell Biol 2004;166:317–323. [PubMed: 15289494]

Boulven I, Robin P, Desmyter C, Harbon S, Leiber D. Differential involvement of Src family kinases in pervanadate-mediated responses in rat myometrial cells. Cell Signal 2002;14:341–349. [PubMed: 11858941]

Brown DA, Rose JK. Sorting of GPI-anchored proteins to glycolipid-enriched membrane subdomains during transport to the apical cell surface. Cell 1992;68:533–544. [PubMed: 1531449]

Caroni P. New EMBO members' review: actin cytoskeleton regulation through modulation of PI(4,5)P (2) rafts. Embo J 2001;20:4332–4336. [PubMed: 11500359]

Chichili GR, Rodgers W. Clustering of membrane raft proteins by the actin cytoskeleton. J Biol Chem 2007;282:36682–36691. [PubMed: 17947241]

Cote JF, Vuori K. GEF what? Dock180 and related proteins help Rac to polarize cells in new ways. Trends Cell Biol 2007;17:383–393. [PubMed: 17765544]

de Diesbach P, Medts T, Carpentier S, D'Auria L, Van Der Smissen P, Platek A, Mettlen M, Caplanusi A, van den Hove MF, Tyteca D, Courtoy PJ. Differential subcellular membrane recruitment of Src may specify its downstream signalling. Exp Cell Res 2008;314:1465–1479. [PubMed: 18316074]

NIH-PA Author Manuscript NIH-PA Author Manuscript NIH-PA Author Manuscript

Etienne-Manneville S. Actin and microtubules in cell motility: which one is in control? Traffic 2004;5:470–477. [PubMed: 15180824]

Fincham VJ, Unlu M, Brunton VG, Pitts JD, Wyke JA, Frame MC. Translocation of Src kinase to the cell periphery is mediated by the actin cytoskeleton under the control of the Rho family of small G proteins. J Cell Biol 1996;135:1551–1564. [PubMed: 8978822]

Gao X, Zhang J. Spatiotemporal Analysis of Differential Akt Regulation in Plasma Membrane Microdomains. Mol Biol Cell. 2008

Hall A. Rho GTPases and the control of cell behaviour. Biochem Soc Trans 2005;33:891–895. [PubMed: 16246005]

Hitosugi T, Sato M, Sasaki K, Umezawa Y. Lipid raft specific knockdown of SRC family kinase activity inhibits cell adhesion and cell cycle progression of breast cancer cells. Cancer Res 2007;67:8139–8148. [PubMed: 17804726]

Holowka D, Sheets ED, Baird B. Interactions between Fc(epsilon)RI and lipid raft components are regulated by the actin cytoskeleton. J Cell Sci 2000;113(Pt 6):1009–1019. [PubMed: 10683149]

Hur EM, Park YS, Lee BD, Jang IH, Kim HS, Kim TD, Suh PG, Ryu SH, Kim KT. Sensitization of epidermal growth factor-induced signaling by bradykinin is mediated by c-Src. Implications for a role of lipid microdomains. J Biol Chem 2004;279:5852–5860. [PubMed: 14630916]

Huyer G, Liu S, Kelly J, Moffat J, Payette P, Kennedy B, Tsaprailis G, Gresser MJ, Ramachandran C. Mechanism of inhibition of protein-tyrosine phosphatases by vanadate and pervanadate. J Biol Chem 1997;272:843–851. [PubMed: 8995372]

Inoue T, Heo WD, Grimley JS, Wandless TJ, Meyer T. An inducible translocation strategy to rapidly activate and inhibit small GTPase signaling pathways. Nat Methods 2005;2:415–418. [PubMed: 15908919]

Jacobson K, Mouritsen OG, Anderson RG. Lipid rafts: at a crossroad between cell biology and physics. Nat Cell Biol 2007;9:7–14. [PubMed: 17199125]

Kaplan KB, Swedlow JR, Varmus HE, Morgan DO. Association of p60c-src with endosomal membranes in mammalian fibroblasts. J Cell Biol 1992;118:321–333. [PubMed: 1378446]

Kasai A, Shima T, Okada M. Role of Src family tyrosine kinases in the down-regulation of epidermal growth factor signaling in PC12 cells. Genes Cells 2005;10:1175–1187. [PubMed: 16324154]

Lasserre R, Guo XJ, Conchonaud F, Hamon Y, Hawchar O, Bernard AM, Soudja SM, Lenne PF, Rigneault H, Olive D, et al. Raft nanodomains contribute to Akt/PKB plasma membrane recruitment and activation. Nat Chem Biol 2008;4:538–547. [PubMed: 18641634]

Lichtenberg D, Goni FM, Heerklotz H. Detergent-resistant membranes should not be identified with membrane rafts. Trends Biochem Sci 2005;30:430–436. [PubMed: 15996869]

Lu S, Ouyang M, Seong J, Zhang J, Chien S, Wang Y. The spatiotemporal pattern of Src activation at lipid rafts revealed by diffusion-corrected FRET imaging. PLoS Comput Biol 2008;4:e1000127. [PubMed: 18711637]

Malinska K, Malinsky J, Opekarova M, Tanner W. Visualization of protein compartmentation within the plasma membrane of living yeast cells. Mol Biol Cell 2003;14:4427–4436. [PubMed: 14551254]

Martin GS. The hunting of the Src. Nat Rev Mol Cell Biol 2001;2:467–475. [PubMed: 11389470]

Maxfield FR, McGraw TE. Endocytic recycling. Nat Rev Mol Cell Biol 2004;5:121–132. [PubMed: 15040445]

Mitra SK, Hanson DA, Schlaepfer DD. Focal adhesion kinase: in command and control of cell motility. Nat Rev Mol Cell Biol 2005;6:56–68. [PubMed: 15688067]

Mukherjee A, Arnaud L, Cooper JA. Lipid-dependent recruitment of neuronal Src to lipid rafts in the brain. J Biol Chem 2003;278:40806–40814. [PubMed: 12912979]

Murakoshi H, Iino R, Kobayashi T, Fujiwara T, Ohshima C, Yoshimura A, Kusumi A. Single-molecule imaging analysis of Ras activation in living cells. Proc Natl Acad Sci U S A 2004;101:7317–7322. [PubMed: 15123831]

Oneyama C, Hikita T, Enya K, Dobenecker MW, Saito K, Nada S, Tarakhovsky A, Okada M. The lipid raft-anchored adaptor protein Cbp controls the oncogenic potential of c-Src. Mol Cell 2008;30:426–436. [PubMed: 18498747]

NIH-PA Author Manuscript

NIH-PA Author Manuscript

NIH-PA Author Manuscript

Pralle A, Keller P, Florin EL, Simons K, Horber JK. Sphingolipid-cholesterol rafts diffuse as small entities in the plasma membrane of mammalian cells. J Cell Biol 2000;148:997–1008. [PubMed: 10704449]

Resh MD. Myristylation and palmitylation of Src family members: the fats of the matter. Cell 1994;76:411–413. [PubMed: 8313462]

Rhee SG. Cell signaling. H2O2, a necessary evil for cell signaling. Science 2006;312:1882–1883. [PubMed: 16809515]

Rodriguez OC, Schaefer AW, Mandato CA, Forscher P, Bement WM, Waterman-Storer CM. Conserved microtubule-actin interactions in cell movement and morphogenesis. Nat Cell Biol 2003;5:599–609. [PubMed: 12833063]

Sandilands E, Brunton VG, Frame MC. The membrane targeting and spatial activation of Src, Yes and Fyn is influenced by palmitoylation and distinct RhoB/RhoD endosome requirements. J Cell Sci 2007;120:2555–2564. [PubMed: 17623777]

Sandilands E, Cans C, Fincham VJ, Brunton VG, Mellor H, Prendergast GC, Norman JC, Superti-Furga G, Frame MC. RhoB and actin polymerization coordinate Src activation with endosome-mediated delivery to the membrane. Dev Cell 2004;7:855–869. [PubMed: 15572128]

Shaner NC, Campbell RE, Steinbach PA, Giepmans BN, Palmer AE, Tsien RY. Improved monomeric red, orange and yellow fluorescent proteins derived from Discosoma sp red fluorescent protein. Nat Biotechnol 2004;22:1567–1572. [PubMed: 15558047]

Shaw AS. Lipid rafts: now you see them, now you don't. Nat Immunol 2006;7:1139–1142. [PubMed: 17053798]

Shima T, Nada S, Okada M. Transmembrane phosphoprotein Cbp senses cell adhesion signaling mediated by Src family kinase in lipid rafts. Proc Natl Acad Sci U S A 2003;100:14897–14902. [PubMed: 14645715]

Simons K, Toomre D. Lipid rafts and signal transduction. Nat Rev Mol Cell Biol 2000;1:31–39. [PubMed: 11413487]

Takahashi H, Suzuki K, Namiki H. Pervanadate-induced reverse translocation and tyrosine phosphorylation of phorbol ester-stimulated protein kinase C betaII are mediated by Src-family tyrosine kinases in porcine neutrophils. Biochem Biophys Res Commun 2004;314:830–837. [PubMed: 14741711]

Thomas SM, Brugge JS. Cellular functions regulated by Src family kinases. Annu Rev Cell Dev Biol 1997;13:513–609. [PubMed: 9442882]

Viola A, Gupta N. Tether and trap: regulation of membrane-raft dynamics by actin-binding proteins. Nat Rev Immunol 2007;7:889–896. [PubMed: 17948020]

Wang Y, Botvinick EL, Zhao Y, Berns MW, Usami S, Tsien RY, Chien S. Visualizing the mechanical activation of Src. Nature 2005;434:1040–1045. [PubMed: 15846350]

Warner AK, Keen JH, Wang YL. Dynamics of membrane clathrin-coated structures during cytokinesis. Traffic 2006;7:205–215. [PubMed: 16420528]

Watson RT, Shigematsu S, Chiang SH, Mora S, Kanzaki M, Macara IG, Saltiel AR, Pessin JE. Lipid raft microdomain compartmentalization of TC10 is required for insulin signaling and GLUT4 translocation. J Cell Biol 2001;154:829–840. [PubMed: 11502760]

Zacharias DA, Violin JD, Newton AC, Tsien RY. Partitioning of lipid-modified monomeric GFPs into membrane microdomains of live cells. Science 2002;296:913–916. [PubMed: 11988576]

Zhang J, Campbell RE, Ting AY, Tsien RY. Creating new fluorescent probes for cell biology. Nat Rev Mol Cell Biol 2002;3:906–918. [PubMed: 12461557]

NIH-PA Author Manuscript

NIH-PA Author Manuscript

NIH-PA Author Manuscript

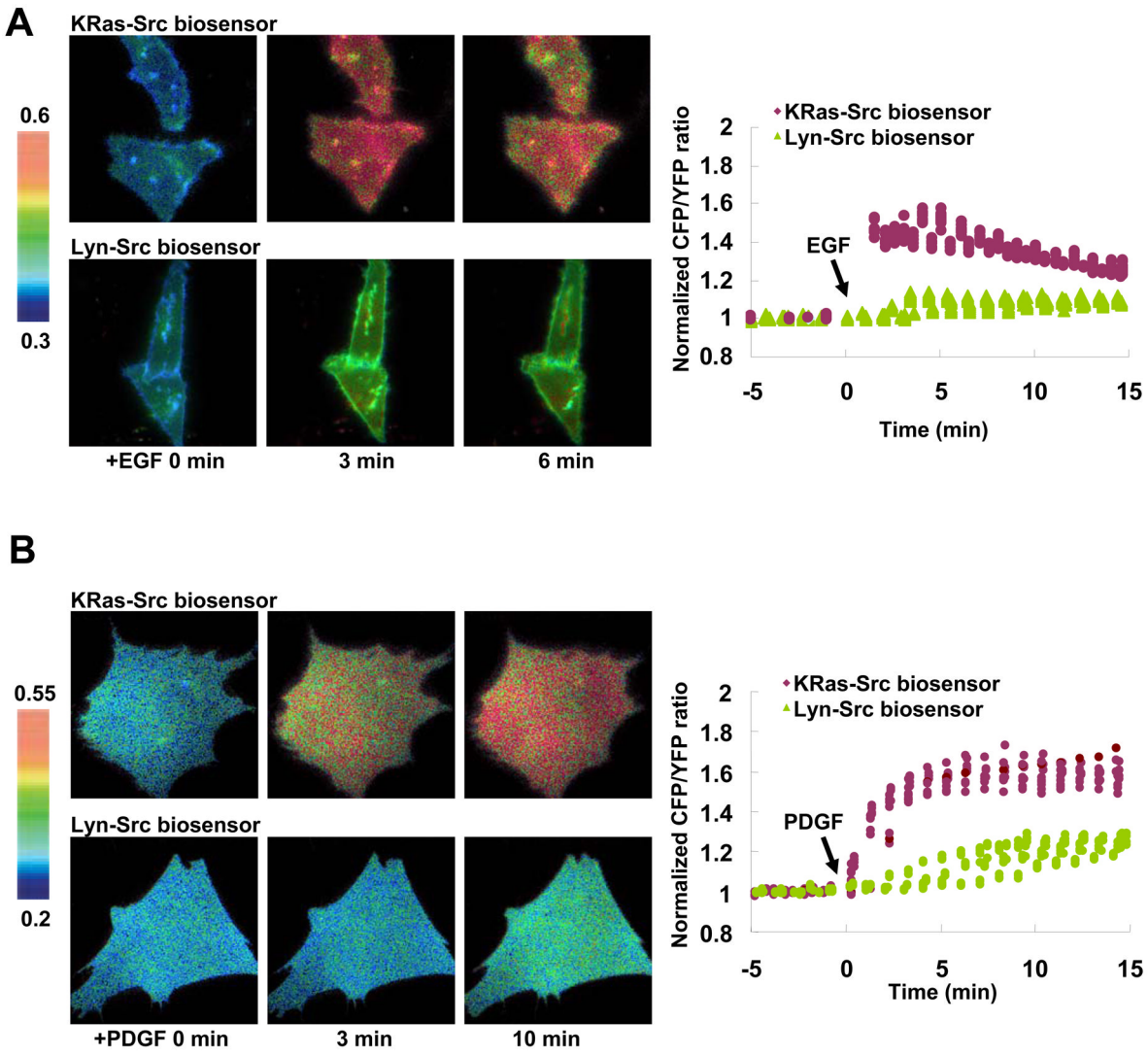

Figure 1. Differential responses of the Src biosensor tethered at different compartments of the plasma membrane upon growth factor stimulations

The CFP/YFP emission ratio images of KRas- (upper panels) or Lyn-Src biosensors (lower panels) in response to 50 ng/ml of (**A**) EGF in HeLa cells or (**B**) PDGF in MEF cells. The scale bars on the left of the images represent the levels of CFP/YFP emission ratio. Time courses on the right panels represent the normalized CFP/YFP emission ratio of KRas- (purple) and Lyn-Src biosensors (green) before and after stimulations.

NIH-PA Author Manuscript

NIH-PA Author Manuscript

NIH-PA Author Manuscript

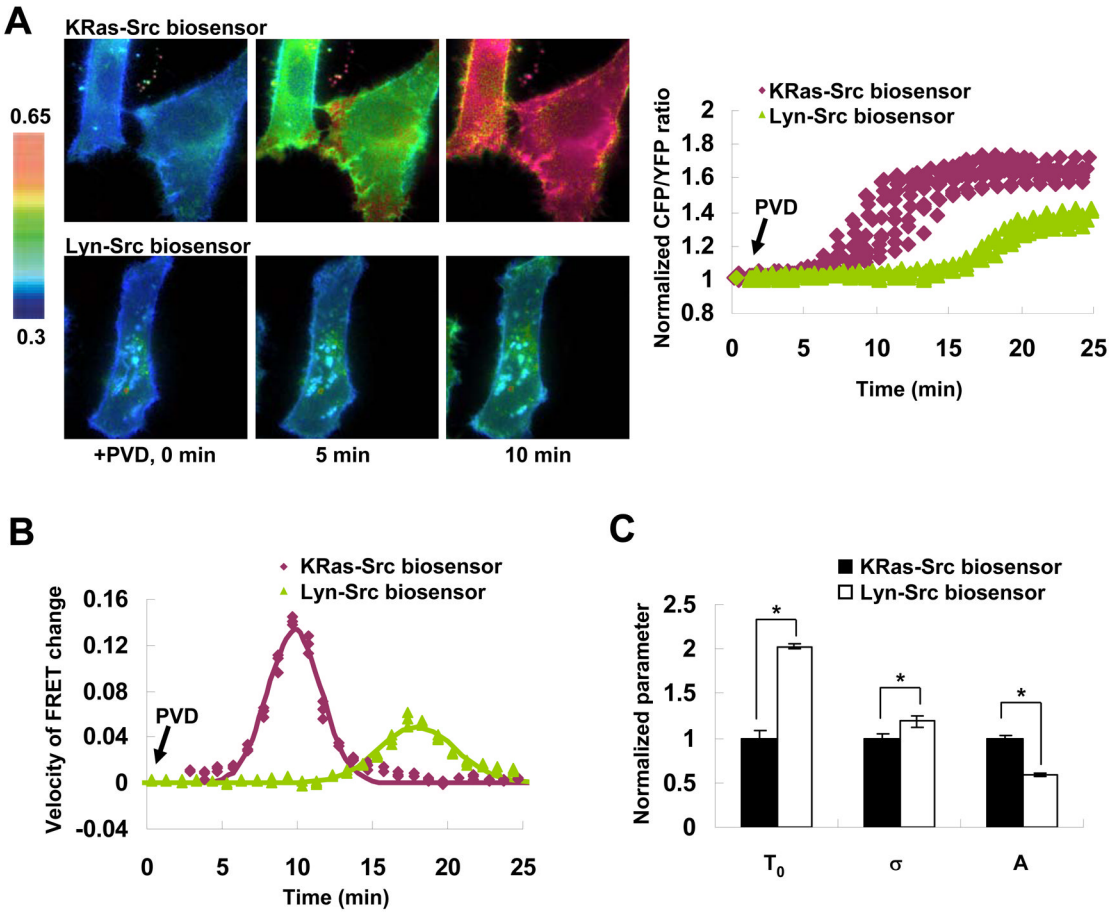

Figure 2. Differential responses of the KRas- and Lyn-Src biosensors upon pervanadate stimulation

(**A**) The CFP/YFP emission ratio images of HeLa cells with KRas- or Lyn-Src biosensors in response to pervanadate (PVD) (left panels). Time courses on the right panel represent the normalized CFP/YFP emission ratio of KRas- (purple) and Lyn-Src biosensors (green) before and after stimulations.

(**B**) The representative velocity curves of FRET signals of KRas- (purple) and Lyn-Src biosensors (green) upon PVD application. Solid lines represent curves of Gaussian function determined by curve-fitting.

(**C**) The normalized values (mean ± SEM) of T_0, σ and A for KRas- (black bar) and Lyn-Src biosensors (white bar) determined by parameter fitting (n=11 and 8, respectively). Asterisks indicate significant differences ($p < 0.05$) between different groups.

NIH-PA Author Manuscript

NIH-PA Author Manuscript

NIH-PA Author Manuscript

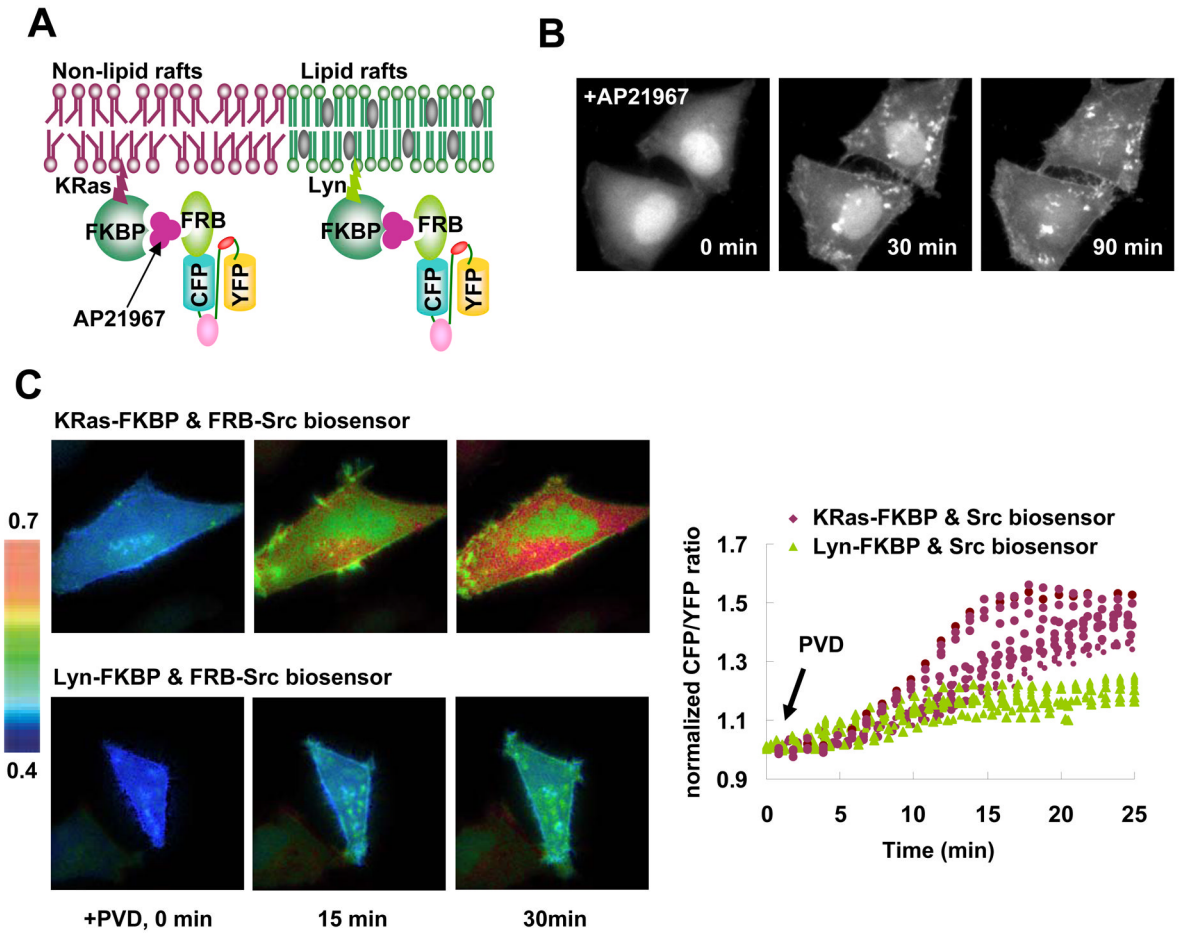

Figure 3. The responses of Src biosensors tethered at the plasma membrane through heterodimerization system

(**A**) A cartoon scheme depicting compartmentalization of the biosensors to the plasma membrane by an inducible heterodimerization system.

(**B**) The CFP images of FRB-Src biosensor before and after AP21697-induced dimerization with Lyn-FKBP.

(**C**) The CFP/YFP emission ratio images of FRB-Src biosensor dimerized with KRas-FKBP or Lyn-FKBP before and after PVD application for various periods of time (left panels). Time courses of CFP/YFP emission ratio of FRB-Src biosensors fused to KRas-FKBP (purple) or Lyn-FKBP (green) upon PVD application in HeLa cells (right panel).

NIH-PA Author Manuscript

NIH-PA Author Manuscript

NIH-PA Author Manuscript

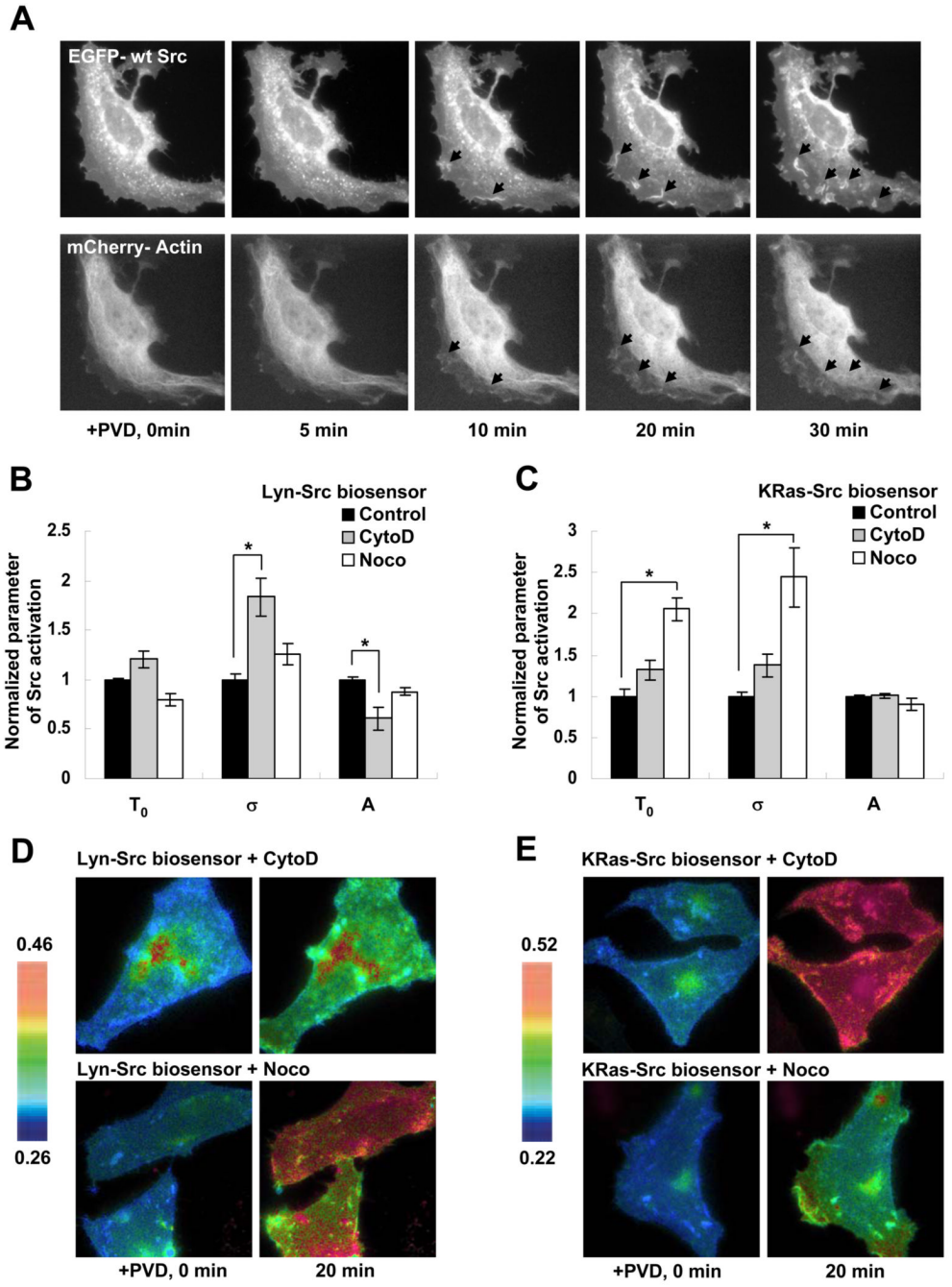

Figure 4. Actin filaments and microtubules differentially regulate the PVD-induced Src biosensor responses at different compartments of the plasma membrane

(**A**) Images of EGFP-conjugated c-Src kinase (upper panels) and mCherry-conjugated β-actin (lower panels) before and after PVD stimulation for various periods of time. Arrows point to the membrane ruffles where Src kinase and actin fibers are colocalized.

(**B** and **C**) Bar graphs represent the normalized values (mean ± SEM) of parameters T_0, σ and A in different groups of (**B**) Lyn- and (**C**) KRas-Src biosensors (n = 8–13). Black, grey and white bars represent results of biosensors in control cells, cells treated with cytochalasin D (CytoD) or nocodazole (Noco). Asterisks indicate significant difference with 95% confidence determined by Bonferroni test.

NIH-PA Author Manuscript

NIH-PA Author Manuscript

NIH-PA Author Manuscript

(**D** and **E**) The CFP/YFP emission ratio images of HeLa cells expressing (**D**) Lyn- or (**E**) KRas-Src biosensors. The cells were exposed to 20 μM of PVD after pretreatment of CytoD (upper panels) or Noco (lower panels) as indicated.

NIH-PA Author Manuscript

NIH-PA Author Manuscript

NIH-PA Author Manuscript

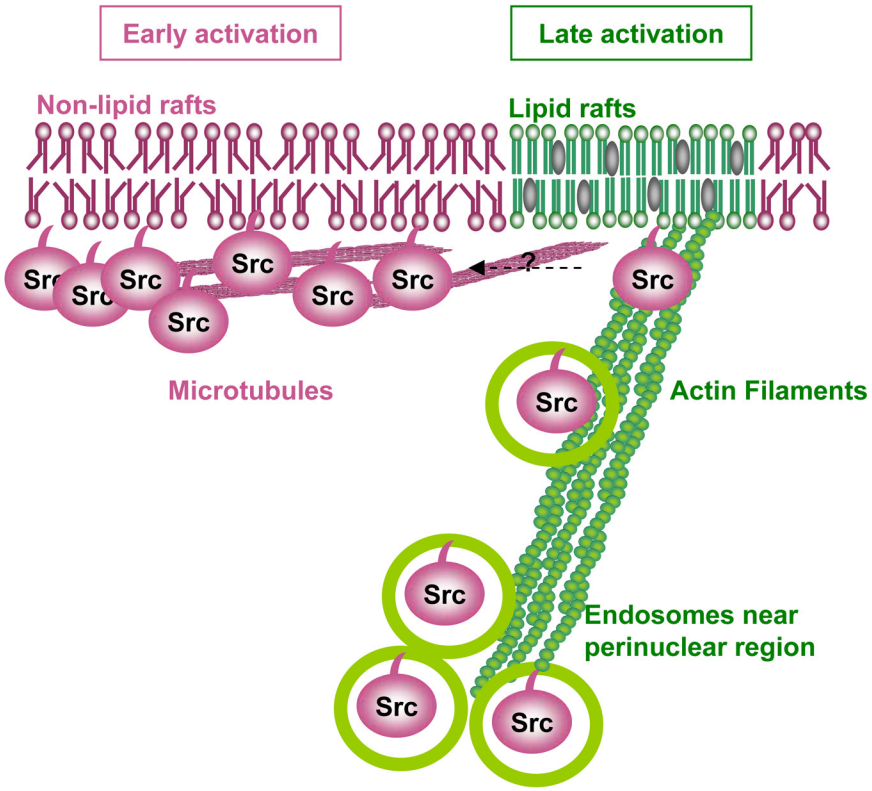

Figure 5. A proposed model of two distinct populations of Src kinases at plasma membrane

One population of Src kinases is pre-stored outside of lipid rafts on plasma membrane at rest state and can be rapidly activated upon stimulation. Another population of Src kinases is located in endosome-like structures around nucleus at rest state, which can translocate to lipid rafts through actin filaments upon stimulation and become activated.